Available online at www.sciencedirect.com
SCIENCE DIRECT
Polymer 46 (2005) 10321–10330
polymer
www.elsevier.com/locate/polymer

Influence of sample thickness on fracture behaviour of a polyketone and a polyketone-rubber blend

W.C.J. Zuiderduin[a], D.P.N. Vlasveld[a], J. Huétink[b], R.J. Gaymans[a,*]

[a]Department of Chemical Technology, University of Twente, P.O. Box 217, 7500 AE Enschede, The Netherlands
[b]Department of Mechanical Engineering, University of Twente, P.O. Box 217, 7500 AE Enschede, The Netherlands

Received 21 April 2005; received in revised form 11 July 2005; accepted 29 July 2005
Available online 24 August 2005

Abstract

The influence of sample thickness on the fracture behaviour of an aliphatic polyketone and a blend of this polymer and 10 wt% core–shell rubber was studied. The sample thickness was varied from 0.1 to 8 mm. The skin morphology was studied by SEM. The fracture behaviour was studied on single edge notch specimen at a high strain rate ($30\ s^{-1}$) in the temperature range of -40 to 120 °C. The fracture stress, fracture strain and fracture energies were determined. The temperature development in the notch area was followed with an Infra Red camera. The cavitation of the rubber particles was studied on tensile bars with a laser setup.

With decreasing specimen thickness the fracture energies increased strongly and the brittle-ductile transition shifted to lower temperatures this both for the aliphatic polyketone and the polyketone-rubber blend. The deformation in these materials in accompanied with a strong temperature increase in the deformation zone. The addition of rubber particles decreases the sensitivity towards the thickness. However, in very thin samples the cavitation of the rubber particles is more difficult and the rubber toughening effect decreases. The strong thickness effects on the fracture toughness indicate for both the homo polymer and the blend indicate that data from a standard test with 4 mm thick samples are not representative for thin walled applications.

Keywords: Thickness; Fracture; Impact

1. Introduction

Aliphatic polyketone terpolymers (PK) are semi-crystalline materials with a glass transition temperature of 15 °C and a melting temperature of 225 °C [1]. The polyketone copolymers behave very similar to polypropylene. These PK are interesting engineering polymers with a high yield stress and a high toughness, however, with a notch they fracture in a brittle manner. Injection moulded products often have a small wall thickness. Thickness influences the stress state within the material is therefore an important parameter in the fracture behaviour.

It is well known that the material in a thick notched plate crazes more easily due to the more severe plane strain stress state ahead of the notch [2]. In a thinner plate the stress state is less severe and can become plane stress. Under plane stress conditions the deformation of the material is easier and more energy can be absorbed. Transition from plane strain to plane stress can be obtained by changing the specimen geometry, strain rate and/or test temperature [2,3]. One method of studying the fracture behaviour at high strain rates is by deforming a Single Edge Notch specimen in a tensile machine. In such a specimen just ahead of the notch, the centre region is in plane strain while the surface region is in plane stress (Fig. 1).

With decreasing the sample thickness the influence of the centre region on the deformation decreases with as a result a gradual change in deformation behaviour. If the samples are tested at high strain rates and with plastic deformation, isothermal conditions are not maintained [4–6]. This non isothermal behaviour complicates studying the thickness effects under impact conditions.

The influence of sample thickness on several polymer systems has been studied before and the general trend is that

* Corresponding author. Address: Department of Science and Technology, University of Twente, P.O. Box 217, 7500 Enschede, The Netherlands.
E-mail address: r.j.gaymans@utwente.nl (R.J. Gaymans).

0032-3861/$ - see front matter © 2005 Elsevier Ltd. All rights reserved.
doi:10.1016/j.polymer.2005.07.107

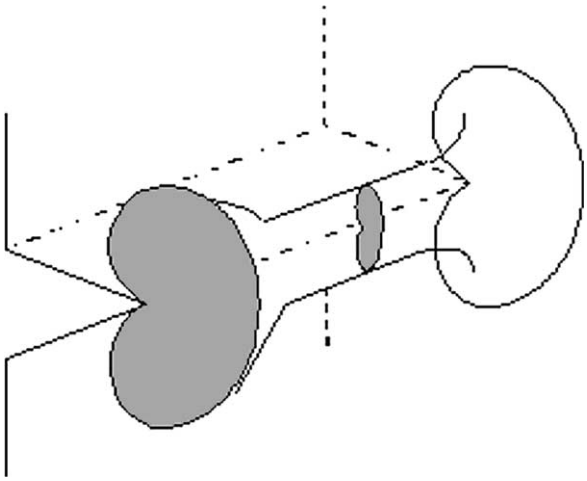

Fig. 1. Shape of the plastic zone in a notched specimen.

with decreasing thickness the fracture toughness increases [7–10].

An important feature of fracture behaviour at high strain rates of ductile polymers is this discontinuous transition from brittle to ductile fracture. So has Polycarbonate a brittle–ductile transition temperature (T_{bd}) which decreases with decreasing sample thickness [11].

Engineering thermoplastics are toughened with rubber particles. Semi crystalline polymers are often semi ductile and in these materials the role of the rubber particles is to cavitate and thereby change the stress state of the matrix material in the neighbourhood of the cavitated particle [12–14]. In this way the sensitivity towards crazing is reduced and shear yielding of the matrix polymer is more likely to take place. The influence of sample thickness with rubber modified blends is interesting as the effectiveness of the rubber also depends on the sample thickness. In thick specimens the stress situation is plane strain and cavitation of rubber particles can easily take place. However, in thin samples with a plane stress situation the cavitation of the rubber particles is difficult. Thus it might be expected that rubber toughening is not as effective in thin samples as it is in thicker applications. Inberg et al. [11] indicated that thickness had a large effect on the fracture properties of PC/ABS blends. The thin specimens the PC/ABS blend started to behave like a PC, it was suggested that at thin specimens the triaxial stress state was not present and therefore cavitation of the rubber phase could not occur. The cavitation behaviour of rubber particles can be studied by dilatometry [15] and by measuring the stress whitening [14]. This last method is a non contacting method that can be used at relative high strain rates.

In this paper, the influence of specimen thickness on the fracture behaviour is studied for a polyketone terpolymer as well as for a blend of polyketone with 10 wt% core–shell rubber particles (PK_{90}–CSR_{10} blend). A single edge notch tensile impact test was used at a high strain rate (30 s^{-1}), over a wide temperature range (−40 to 120 °C). The fracture behaviour of the notched samples has been quantified in terms of deformation before crack initiation, stress at crack initiation and deformation during crack propagation and total fracture energy [6]. Also studied were the cavitation of the rubber particles and the temperature development in the notch area.

2. Experimental

2.1. Materials

Polyketone terpolymer (Carilon P1000) was kindly supplied by SHELL, Amsterdam, The Netherlands. The polyketone is a perfect alternating terpolymer, polymerised from ethylene and carbon monoxide; 6 mol% of the ethylene is replaced by propylene to lower the melt temperature. The polyketone has a glass transition temperature of approximately 15 °C and a melting temperature of 225 °C with a crystallinity of 35 wt% and its density is 1.24 g cm^{-3}. A core–shell rubber (CSR) (Blendex 338) with a particle size of 200 nm was kindly supplied by GE Plastics, Bergen op Zoom, The Netherlands. The core is of polybutadiene and the shell of SAN.

2.2. Specimen preparation

Compounding of the blend with 10 wt% CSR (PK_{90}–CSR_{10}) was done using a Berstorff (ZE 25×33D) co-rotating twin screw extruder. In the extrusion step, barrel temperatures were set at 240 °C and a screw speed of 140 rpm was maintained. The throughput was approximately 4 kg h^{-1}.

The PK and the PK_{90}–CSR_{10} blend were injection moulded into rectangular bars (74×10×thickness) using an Arburg Allrounder 221-55-250 injection moulding machine. Moulds of 8, 4, 3, 2, 1.5 and 1 mm depth were used. The barrel had a flat temperature profile of 240 °C, the mould temperature was kept at 70 °C with an injection pressure of 55 bar and the holding pressure of 45 bar. A single-edge V-shaped notch of 2 mm depth and tip radius 0.25 mm was milled in the moulded specimens.

A Wickert WLP 1600/5×4/3 press was used to press 0.1 and 1 mm thick sheets of PK, and PK_{90}–CSR_{10} blend at 200 bar and 240 °C. Rectangular strips of 10×74 mm were cut from the sheets with a scalpel with a fresh blade for each specimen. A notch was milled in the strips after clamping them between two thick specimens.

2.3. Single edge notched tensile impact experiments

The fracture behaviour at high test speeds was studied by a tensile test on notched bars, referred to as single edge notch tensile impact test (SENTI). Tests were carried out on

a Schenck VHS servo hydraulic tensile machine. The piston displacement was kept at 1 m s^{-1}. The specimen length between the clamps was 35 mm, thus accordingly the macroscopic apparent strain rate was 30 s^{-1}. A pick up unit is used to allow the piston to reach the desired test speed before loading the specimen. All moving parts are made of titanium in order to diminish inertia effects. The contact between the pick-up unit and the lower clamp is damped by a rubber pad in order to reduce harmonic oscillations [16]. The force is measured with a piezo-electric force transducer located between the upper clamp and the crosshead. Force, time and piston displacement are recorded using a transient recorder with a maximum sample rate of 2 MHz per channel. After completion of the test the results are sent to a computer. The data from the high speed SENTI test were condensed to: Maximum stress, the strain at maximum stress (the initiation strain), the strain after the maximum stress (the propagation strain) and the energy to fracture. All experiments were performed in five-fold. Typical SENTI graphs for both a brittle and a ductile fracturing sample are given in Fig. 2.

2.4. Infrared thermography

The temperature rise during fracture of specimens of thickness 1–4 mm in a SENT test was monitored using an infrared camera. Camera specifications are listed in Table 1. With the infrared camera, only temperatures at the surface of the specimen can be determined. The spot size of about 100 μm which is large compared to the fracture zone size. The temperature indicated in one spot is an average temperature over the entire spot size. The temperature can, therefore, not be determined directly at the fracture surface, which is expected to be highest.

As the response time of the camera is not so high the SENT tests were carried out at a low strain rate (0.03 s^{-1}).

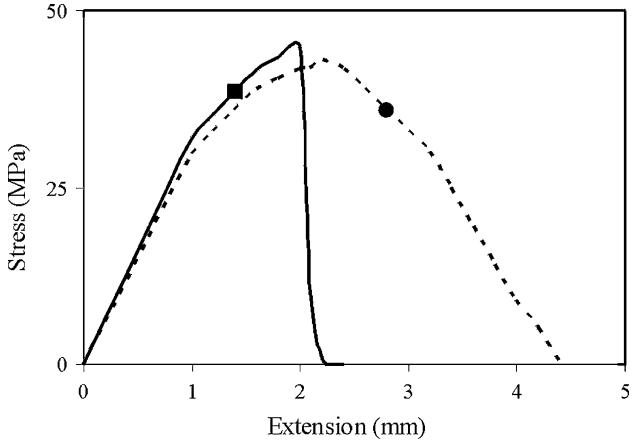

Fig. 2. Single edged notched tensile impact (SENTI) curves for a brittle PK (■) and a ductile PK (●).

Table 1
Technical data for the infrared camera, equipped with close-up lens

TVS 600 AVIO Nippon Avionics Co., Ltd	
Temperature range	−20 to 300 °C
Temperature resolution	0.15 °C
Spectral range	8–14 μm
Image rate	30 frames s^{-1}
Spatial resolution	0.1 mm spot size

2.5. Onset of cavitation of rubber particles in a matrix polymer [14]

The cavitation measurements were performed on injection moulded tensile samples with a Schenck Hydropulse 25 VHS high speed hydraulic tensile tester. The principle of the method is that cavitation in a blend is accompanied by a change in transparency due to stress whitening. The stress whitening is caused by the scattering of the incident light by cavitated particles. By measuring the transmittance of light the onset of stress whitening (cavitation) can be determined. The intensity of the transmitted light will drop suddenly and this lowering of the intensity can be detected by a photodiode placed on the other side of the specimen. As light source a helium-neon laser with a maximum output power of 30 mW and a wavelength of 633 nm was used. The data were sampled using a transient data recorder after which the data was transferred to a computer set-up. The strain rate in this test was 0.01 s^{-1}.

Determination of cavitation by this method also has the advantage that it is a non contacting method that can even be used at relative high strain rates.

2.6. Scanning electron microscopy

Scanning electron microscopic (SEM) pictures were taken to study the morphology of the materials. SEM specimens were prepared by cutting with a CryoNova microtome at −120 °C using a diamond knife (−110 °C) and cutting speed of 1 mm s^{-1}.

This smooth surface was then chemically etched using a permanganic etchant. The etchant consist of 0.4 g potassium permanganate dissolved in 4 ml distilled water to which was then added 16 ml of concentrated phosphoric acid. The samples and etchant were placed on a resonating plate to reduce the built up of residues. After etching (typically 1 h) the samples were washed in three consecutive baths of (1) 30% aqueous hydrogen peroxide, (2) distilled water and (3) acetone. At least 1 min in each bath. These samples were then coated with a gold layer and studied with a scanning electron microscope (SEM).

3. Results and discussion

The influence of thickness on the fracture behaviour has been studied for an aliphatic polyketone (PK) and for a

blend of PK and 10% core–shell rubber. Samples of different specimen thickness were prepared with injection moulding (1–8 mm) and compression moulding, (1 and 0.1 mm). The results of the 1 mm compression moulded and injection moulded samples were very similar, therefore only the results of the 1 mm specimen on the injection moulded series are shown here.

The deformation behaviour was studied on single edged notch samples in tensile at high test speeds. This single edged notched tensile impact (SENTI) test was also used as thin samples in notched Izod or notched Charpy tests bend away. The SENTI tests were carried out at 1 m s^{-1} piston displacement, which comes down to an apparent strain rate of 30 s^{-1}. This strain rate is comparable to the strain rate in a notched Izod and notched Charpy test. The SENTI test is carried out at different temperatures.

It was not possible to obtain SENTI test stress–strain data for the 0.1 mm thin compression moulded films, as the films could not bear the weight of the clamp. Therefore, the 0.1 mm film was clamped in together with a 1 mm specimen. Unfortunately, in this way only the brittle–ductile transition temperature can be determined and this visually from the fracture surface. It was assumed that the presence of the 1 mm specimen did not influence the fracture processes in the thin film. Samples that have fractured brittle have a translucent fracture surface and samples that have fractured ductile have a white fracture surface.

3.1. Polyketone

It is known that with injection moulding of semi crystalline polymers a skin-core morphology is often formed. The skin layer has a different spherulitic structure. The cross section of a 2 mm thick sample was etched and the morphology studied with SEM. The structure of a 1 mm thick sample in the middle (Fig. 3(a)) and at the surface (Fig. 3(b)) is given. The spherulitic size in this sample is 5–10 μm and structure near the surface (Fig. 3(b)) is very similar to in the middle (Fig. 3(a)) of the sample. A 'skin layer' can hardly been seen and the size of the skin is less than the size of the spherulites. The specimen with other sample thicknesses had similar morphologies. The skin size in PK-polymer samples is very small and much smaller than the specimen thicknesses we study. The skin structure is thus not expecting to play a role in the deformation behaviour of our notched samples.

3.1.1. SENTI

Single edged notched tensile impact test were carried out and the data have the form as given in Fig. 2. The crack initiation is assumed to take place at the point of maximum stress. For low strain rates this was verified and the onset of crack initiation always coincides with the point of maximum stress. Determent was the displacement up to crack initiation, the maximum stress, the displacement after the maximum load and the total fracture energy. Brittle fracture is characterised by zero propagation displacement (and energy). The onset ductile fracture is defined as there where the propagation displacement started to increase and thus where additional energy is supplied to propagate a crack through the specimen. This onset is called the brittle–ductile transition.

3.1.1.1. Maximum stress. The maximum stress (fracture stress) was measured as a function of test temperature at different specimen thickness (Fig. 4(a)). The general trend is that maximum stress decreased with increasing temperature. This decrease in fracture stress is due to a decrease in yield and craze stress at higher temperatures.

The maximum stress also decreased with increasing thickness. So is the maximum stress at 20 °C about 70 MPa at 1 mm thickness (ductile) and about 45 MPa at 8 mm thickness (brittle). In the thick specimen a more developed plane strain stress state exists, leading to crack initiation at

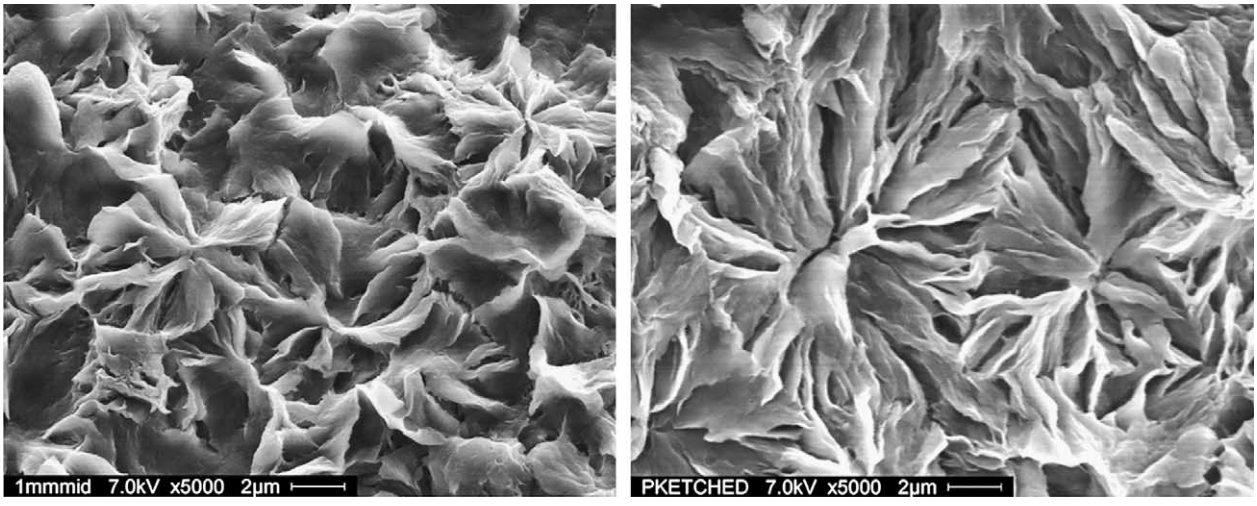

Fig. 3. SEM micrographs of an etched 1 mm injection moulding bar: (a) in the middle; (b) near the surface.

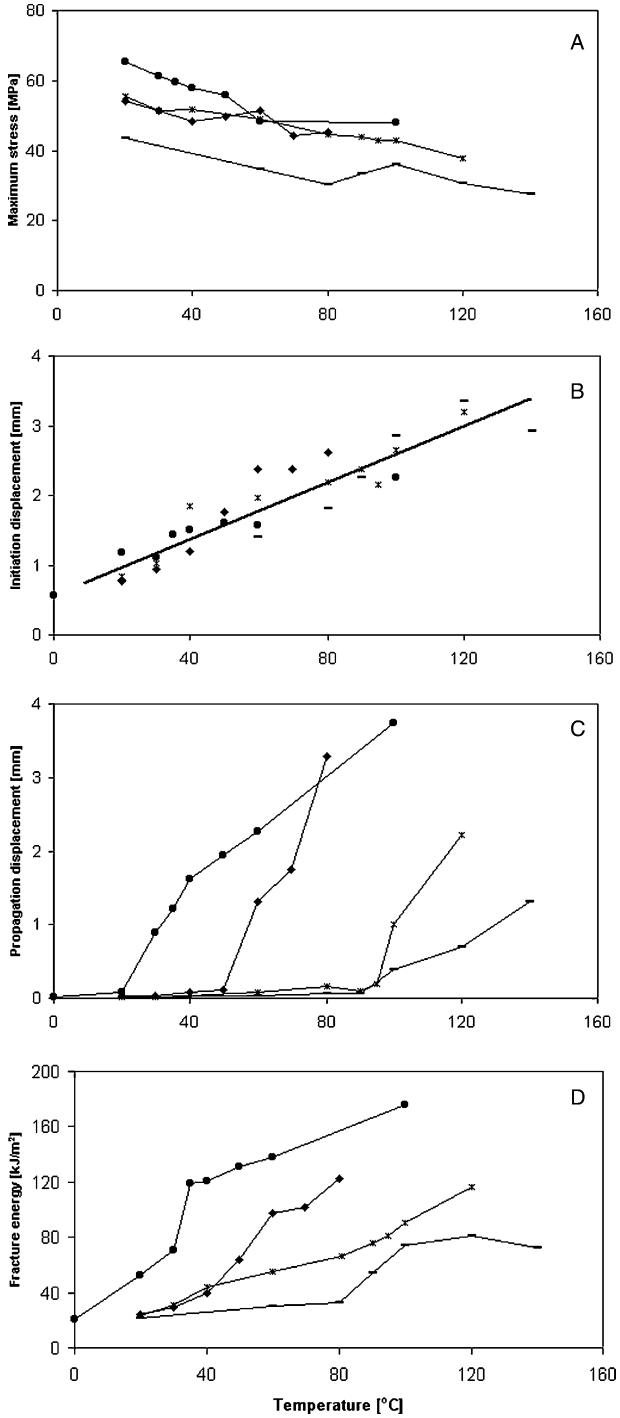

Fig. 4. SENTI data for PK, at 30 s^{-1}, maximum stress, crack initiation displacement, crack propagation displacement and fracture energy as a function of temperature : (●) 1 mm; (♦) 2 mm; (*) 4 mm; (–) 8 mm.

lower macroscopic stress level. In thin specimens the plane stress state prevails, and the specimen can be loaded to higher stresses before craze formation will take place. At elevated temperatures the differences become smaller. The maximum stress data do not show a brittle–ductile transition.

3.1.1.2. Crack initiation. Crack initiation displacement, defined as clamp displacement up to maximum force, was determined (Fig. 4(b)). The crack initiation displacements (and crack initiation energies) increased strongly with temperature. The crack initiation displacement was under the studied conditions independent of failure mode (brittle or ductile fracture). The temperature is an important parameter for the crack initiation process.

The crack initiation displacements do not show a great dependence on specimen thickness. The thinner samples have somewhat higher crack initiation values. The effect of the thickness is at low temperatures relatively larger. This is in line with the maximum stress data (Fig. 4(a)).

The crack initiation deformation is partly due to the straining of the whole sample. A lowering of the plain strain state increases the maximum stress and with that the total deformation in the sample.

Ahead of the notch plastic deformation takes place and most of this plastic deformation energy is dissipated as heat. This heat development was studied with infrared thermography at a strain rate of 0.03 s^{-1}. The size of the heated zone decreases with specimen thickness (Fig. 5(a)). The zone size was for the 1 and 8 mm thick samples, 2 and 0.2 mm. Thus as function of sample thickness considerable differences in deformation in the notch area is taking place but this is only partly reflected in the crack initiation displacement values.

3.1.1.3. Crack propagation. Crack propagation displacement is defined as clamp displacement from maximum force to fracture. As the crack initiation is taking place at the maximum stress, the crack propagation displacement is the deformation during fracture. If a sample fractures in a brittle manner than the crack propagation displacement is minimal, however, with ductile tearing the propagation displacement can be large. The crack propagation displacement data are given in Fig. 4(c). The crack propagation displacements show a similar dependency on temperature for all specimen thicknesses. At low temperatures the displacement necessary to propagate a crack is close to zero. At a certain temperature the crack propagation displacement starts to rise steeply with temperature and there is no levelling off at higher temperatures However, with increasing specimen thickness the onset of ductility (brittle–ductile transition) is shifted to higher temperatures. The specimen thickness has a large influence on the crack propagation process; a thinner sample shows a ductile response at much lower temperatures compared to specimen with a relative thick dimension. The onset of ductility (the brittle–ductile transition) shifts from 20 up to 100 °C upon increasing the specimen thickness from 1 to 8 mm. The crack propagation displacement is mainly from the deformation in process zone next to the fracture zone, but ahead of the running crack. The elastic contribution of the rest of the sample present at the onset of fracture is during fracture lowered due to the decreasing stress in the sample. This elastic

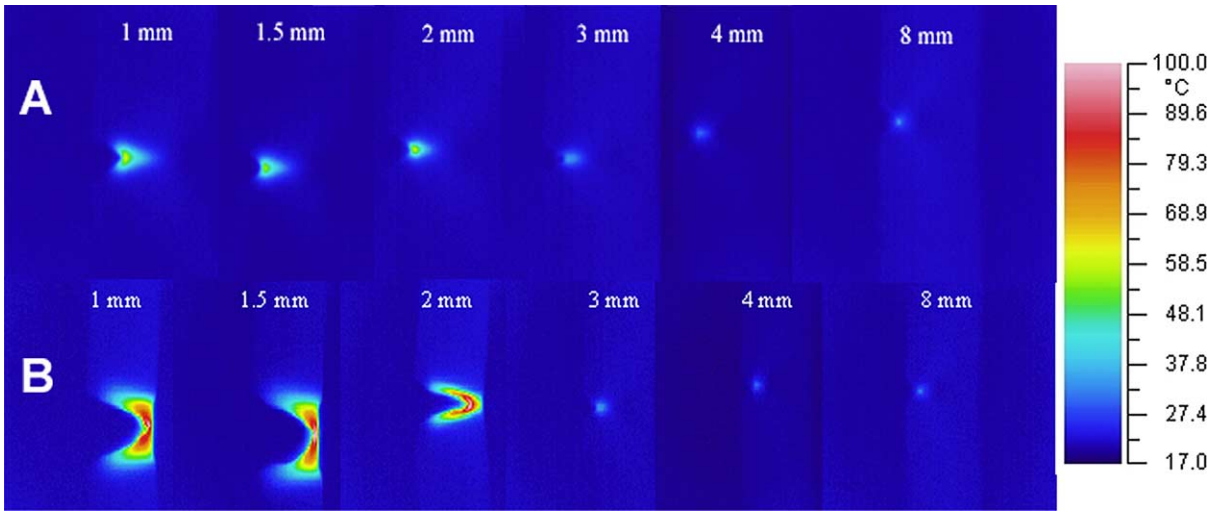

Fig. 5. Thermograph of the plastic zone (IR data) for PK, SENT, 0.03 s^{-1}, 20 °C during the fracture process for different specimen thickness,: (a) before crack initiation; (b) after crack initiation.

energy in the rest of the sample is now dissipated in the process zone. The steep rise in crack propagation displacement with temperature suggest that in the ductile mode the material in the process zone is more and more deformed and/or more material is taking part in the deformation with as a result a thicker process zone.

The temperature development in the process zone was also studied with infrared thermography (Fig. 5(b)). The crack propagation (at 20 °C) was only for the 1 and 2 mm samples slow enough to be measured. The zone size decreased in going from 1 to 2 mm thick samples and this is in line with the crack propagation data. A maximum surface temperature of 100 °C was recorded. Extrapolating this to the high strain rates (30 s^{-1}) a temperature of ~185 °C can be expected [17]. This temperature is approaching the melting temperature of PK. In the brittle fracturing thick samples the temperature still increased to 33 °C. Even here the deformation is thus not isothermally.

3.1.1.4. Fracture energy. The total amount of fracture energy is obtained by integrating the force–displacement curve. The energy necessary to fracture the specimen increased with temperature for all specimen thicknesses (Fig. 4(d)). With temperature the maximum stress decreased but the initiation and propagation displacements increased and their increase is stronger than the decrease in the maximum stress. With increasing specimen thickness the fracture energy decreased and this both at low and high temperatures. This decrease is mainly due to the decreasing crack propagation displacement. The fracture energies for the PK polymer are thus strongly dependant on both the sample thickness and the temperature. The temperature

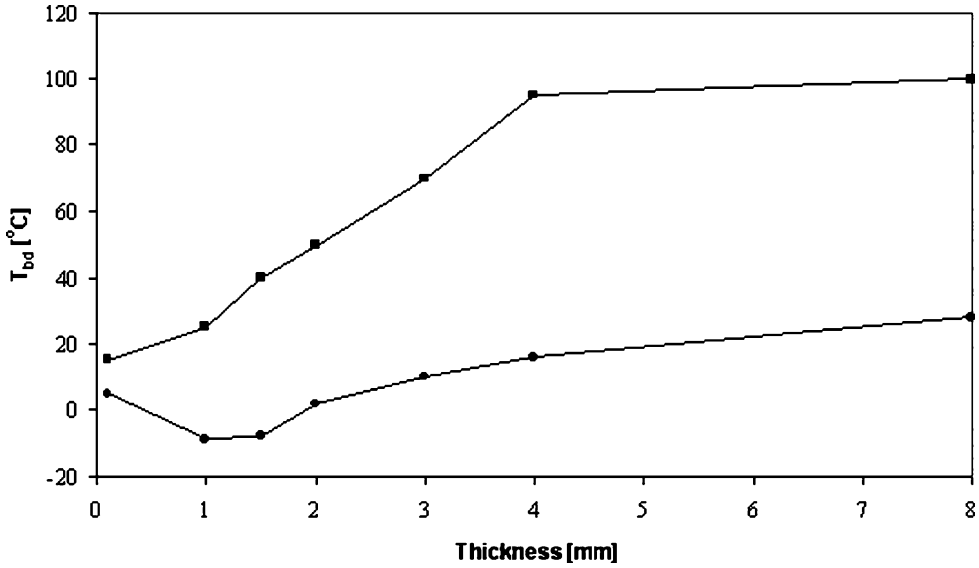

Fig. 6. The brittle–ductile transition temperatures (T_{bd}) as a function of specimen thickness at 30 s^{-1}: (■) PK; (●) PK_{90}–CSR_{10} blend.

dependence is similar to that observed on polypropylene [18]. The transition from ductile to brittle is also visible in the fracture energy data and this transition is shifted with thicker samples to higher temperatures. These brittle–ductile transition temperatures here coincides with the transition temperatures as obtained from the crack propagation displacements. The brittle–ductile transition of the 0.1 mm thick film is obtained by looking at the fractured samples. The brittle–ductile transition temperature (T_{bd}) increases with specimen thickness (Fig. 6).

In the region 1–4 mm thick PK samples the T_{bd} increase linearly with the sample thickness. The 8 mm samples had a similar T_{bd} as the 4 mm samples. These results suggest that in the thickness range 1–4 mm the deformation is very sensitive to the sample thickness. It is evident that the specimen thickness has a large influence on the fracture behaviour of PK, PC [11] and probably also on other polymers like PP and PA.

3.2. PK–CSR-blend

Of improving the toughness, polymers are often blended with rubber [19]. The main effect of increasing the rubber content in semi-ductile polymers is the shift in T_{bd} to lower temperatures. This trend was also observed with the PK polymer modified with core–shell rubber particles [17]. Studied is now the effect of specimen thickness on the deformation behaviour of a PK_{90}–CSR_{10} blend. The function of the rubber in a blend of a semi-ductile polymer is to cavitate at a high stress. The cavitation releases the triaxial stress state in the neighbourhood of the cavities and lowers thereby the sensitivity towards crazing. In fracturing blends, the cavitation of the rubber particles as well as subsequent yielding of the matrix polymer absorbs energy, but the yielding of the matrix polymer is the dominant energy consuming mechanism [19].

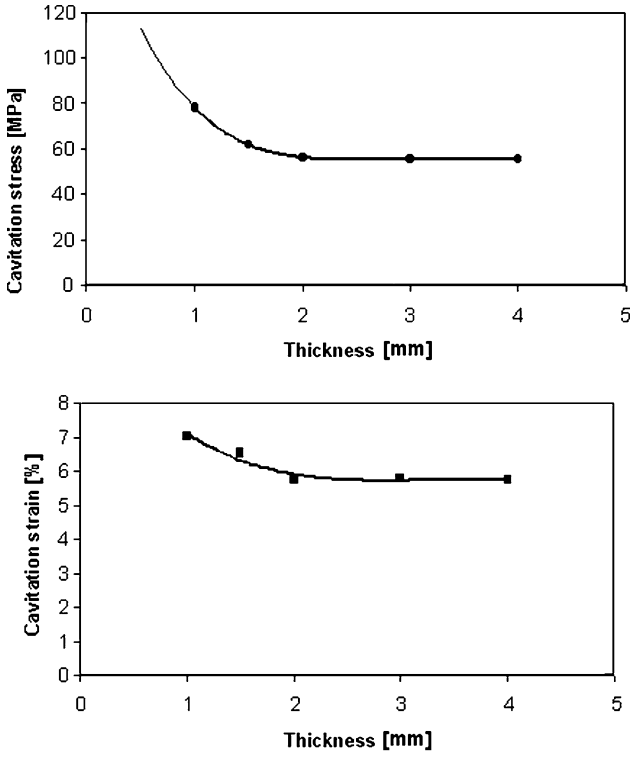

Fig. 7. Macroscopic cavitation stress and strain of PK_{90}–CSR_{10} blend in tensile 20 °C, (0.01 s^{-1}) as a function of specimen thickness.

SENTI tests are performed on specimen with varying thickness of 0.1 up to 8 mm and the temperature was varied. The piston speed was kept at 1 m s^{-1}, which corresponds well with the velocity during an Izod impact test. The macroscopic apparent strain rate based on the clamping distance is then calculated to be 30 s^{-1}.

3.2.1. Influence of specimen thickness on the rubber cavitation process

The function of the rubber in a blend is to cavitate and thereby to change the stress state. The cavitation of particles is accompanied by stress whitening. The onset of stress whitening was studied by measuring the light transmittance in a tensile bar with a laser light source in a tensile test. The tensile test bars were deformed at a strain rate of 0.01 s^{-1}, this is a factor 3000 slower than the SENTI test. One must bear in mind that the stress and strain at onset of cavitation is the stress and strain acting on the blend when the rubber starts to cavitate. This stress is not the same as the stress and strain acting on the rubber particles at the onset of cavitation. The cavitation behaviour of a rubber particle is depends on the amount of volume strain on such a particle. In a plane strain stress state the volume strain on a particle will increase linearly with the macroscopic strain. In a mixed mode state, a larger macroscopic strain will then be necessary to create the volume strain to cavitate the particle. In a complete plane stress state, the deformation is without volume change and cavitation of the particles will be improbable.

For the cavitation measurements tensile test bars are used without a notch, the samples were 10 mm width and had different thicknesses of 1–4 mm. The 8 mm samples had a too low transparency for this experiment. The onset of cavitation stress is at a high stress and decreases with increasing sample thickness (Fig. 7(a)). However, between 2 and 4 mm thick samples the effect was minimal. The onset of cavitation strain also decreases with increasing sample thickness (Fig. 7(b)) in a similar way as the onset of cavitation stress.

From these results it can be concluded that the onset of cavitation is for the thick samples at a lower stress and strain. The fact that the 4 mm samples have the same cavitation stress and strain as the 2 mm samples suggests that at these strain rates above a sample thickness of 2 mm the plane strain state is dominant. Below 2 mm there is an increase in both stress and strain at the onset of cavitation. The plane stress state is becoming more important at these thin samples and more macroscopic strain is necessary to

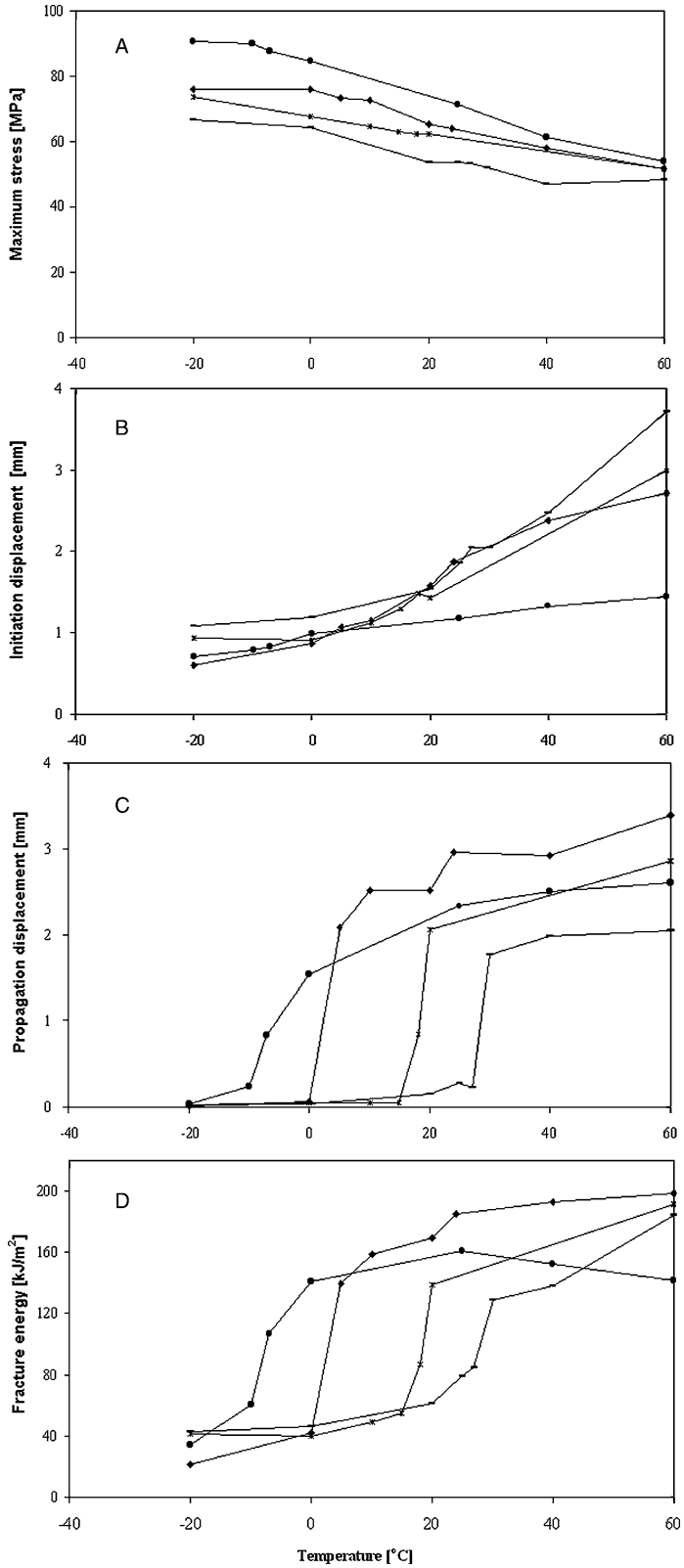

Fig. 8. SENTI data PK-10%CSR, 30 s^{-1}, maximum stress, crack initiation displacement, crack propagation displacement and fracture energy as function of temperature: (●) 1 mm; (♦) 2 mm; (*) 4 mm; (–) 8 mm.

initiate cavitation of the rubber particles. The results suggest that in the thicker tensile samples (>2 mm) (at 20 °C, 0.03 s^{-1}) a plane stress state was present and that cavitation in the thinner samples is more difficult. It can be expected that at the higher strain rates this dependency on the sample thickness is similar.

3.2.2. SENTI

The maximum stress in the SENTI test was also measured on PK_{90}–CSR_{10} blend as function of temperature at different sample thicknesses (Fig. 8(a)). The general trend is that with increasing temperature the maximum stress decreases. Also with increasing sample thickness the maximum stress are lower and this even at high temperatures.

At 60 °C all the blend samples fracture in a ductile way but still there is an effect of the sample thickness. This is an indication that 10 wt% of CSR is not sufficient to release all of the tri-axial stresses, otherwise the maximum stresses should have been equal. A brittle–ductile transition was in the maximum stress data not observed. Surprisingly, the maximum stresses of the PK–CSR blend are somewhat higher compared to the neat PK (Fig. 6(a)) and this particular for the thicker samples. The notch sensitivity is for the blend lower than for the neat PK [6]. The rubber phase suppresses the crazing by changing the stress state of the material surrounding the cavitated rubber particles, this leads to the somewhat higher fracture stresses for the blend material.

3.2.2.1. Crack initiation. The crack initiation energies show the same trend as the crack initiation displacements therefore only the displacement data are discussed here (Fig. 8(b)). The crack initiation strain increases with temperature for all specimen thicknesses. The resistance to crack initiation is larger when the temperature is increased. With increasing temperature the yield stress is decreased and therefore the material is able to deform easier.

At low temperatures the crack initiation displacements do not show much difference. At elevated temperatures the thinnest samples show much lower initiation displacements then the thicker samples. The 1 mm thick samples of the PK–CSR blend show even lower crack initiation displacements compared to the neat PK. One aspect playing an important role in this is the stress state in the sample. The thinner sample is less constrained and therefore cavitation of the rubber particles is more difficult. When the rubber phase does not cavitate, the particles act as a stress concentrators and as a result the initiation strain is reduced.

3.2.2.2. Crack propagation. The crack propagation displacements show S-curves with a jump in propagation displacement at the brittle–ductile transition (Fig. 8(c)). With increasing sample thickness the S-curve is shifted to higher temperatures indicating a shift in the brittle–ductile transition temperature (T_{bd}) with sample thickness. The thicker specimen show a higher T_{bd}, apparently the cavitation of the rubber particles is not able to compensate fully for the more severe stress state in the thicker sample. A reason for this could be that the 10% rubber particles is not sufficient to release the elastic constrain fully. Also remarkable is that at high temperatures in the ductile fracturing mode the thicker samples have a lower fracture displacement. The 1 mm samples have a low T_{bd} but the propagation displacement is not so strong.

The process zone was also studied by measuring the temperature development in this zone with infrared thermography (Fig. 9) at a strain rate of 0.03 s^{-1}.

The deformation zone size hardly changed with thickness and also radius of the running crack is similar for all specimen thicknesses. The maximum temperature was for the 1 mm sample 70 °C and for the thicker samples 90 °C.

3.2.2.3. Fracture energy. The fracture energy clearly shows S-type curves with a sharp brittle–ductile transition (Fig. 8(d)). The impact energy increases with a factor of 5 over this transition. With increasing sample thickness the S-curves shifted to higher temperatures. At very low temperatures in the brittle region the fracture energies are for all samples similar. In the ductile region at high temperatures the fracture energies decreases with increasing sample thickness. The 1 mm thick specimen behaves somewhat different at elevated temperatures as the fracture energy decreased with temperature. This effect is might be due to difficulty of cavitation of the rubber particles in the 1 mm samples and particular at high temperatures.

The T_{bd} decreases with decreasing sample thickness. However, the thinnest specimens (0.1 and 1 mm) do not show a further lowering in the transition temperature. This is probably due to a less favourable stress state for cavitation

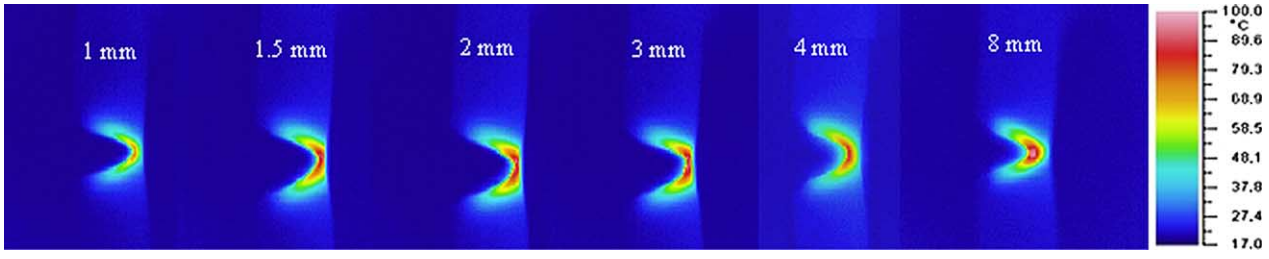

Fig. 9. Thermograph of the plastic zone (IR data) for PK_{90}–CSR_{10} blend, SENT, 0.03 s^{-1}, 20 °C during the fracture.

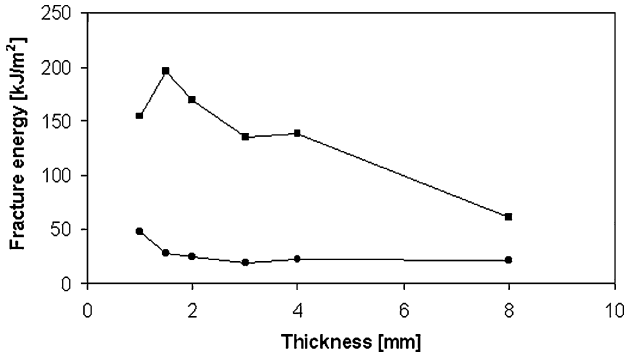

Fig. 10. Fracture energy as a function of specimen thickness in SENTI ($30\ s^{-1}$) at 20 °C: (●) PK; (■) PK_{90}–CSR_{90}.

in the thin samples. The T_{bd} of the blend is much lower than that of the neat polymer and this particular for the thicker samples. However, at very small thicknesses (0.1 mm) the differences between the blend and PK in T_{bd} become small.

The fracture energies (at 20 °C) decreases drastically with increasing sample thickness (Fig. 10). This decrease is partly due to the change in ductile-to-brittle mode of deformation. The 1 mm sample has a lower fracture energy that the 1.5 mm sample. The neat PK samples have much lower fracture energies and this is partly due to the fact that the neat samples fracture in a brittle mode.

It is evident from Fig. 6 that the sensitivity towards specimen thickness is reduced considerably by adding a heterogeneous rubber phase. The cavitated rubber phase depresses the initiation of crazes and decreases the growth rate of crazes. The effect is stronger at the thicker specimen. The rubber cavitation decreases the amount of plane strain in the sample.

4. Conclusions

These results show that the thickness has a large influence on the impact resistance of a material. Both the polyketone and the rubber blend become more impact resistant at thinner geometry's. The fracture energies increases and the brittle–ductile transition shift to lower temperatures. The addition of a heterogeneous rubber phase decreases the sensitivity towards the thickness but in thinner samples the cavitation of the rubber particles is limiting. The fracture stresses and the fracture energies are for the blend material larger. The fracture behaviour is strongly dependant on the temperature. Puzzling is still what the effect is of the temperature development in the samples on the fracture behaviour. These results suggest that a standard test with 4 mm thick samples is not representative for thin walled applications.

References

[1] Zuiderduin WCJ, Homminga D, Huétink J, Gaymans RJ. Polymer 2003;44:6361.
[2] Mills NJ. J Mater Sci 1976;11:363.
[3] Hertzberg RW. Deformation and fracture mechanics of engineering materials. New York: Wiley; 1989.
[4] Williams JG. Adv Polym Sci 1978;27:67.
[5] Zuiderduin WCJ, Huétink J, Gaymans RJ. J Appl Polym Sci 2003;91:2558.
[6] Yap OF, Mai LW, Cotterell B. J Mater Sci 1983;18:657.
[7] Fernando PL, Williams JG. Polym Eng Sci 1980;20:215.
[8] Chan MKV, Williams JG. Polym Eng Sci 1981;21:1019.
[9] Hobbs SY, Bopp RC. Polymer 1980;21:559.
[10] Yee AF. J Mater Sci 1977;12:757.
[11] Inberg JPF, Gaymans RJ. Polymer 2002;43:3767.
[12] Donald AM, Kramer EJ. J Mater Sci 1982;17:1765.
[13] Yee AF, Pearson RA. J Mater Sci 1986;21:2462.
[14] Dijkstra K, van der Wal A, Gaymans RJ. J Mater Sci 1994;29:3489.
[15] Karger-Kocsis J, Csikai I. Polym Eng Sci 1987;27:241.
[16] Béguelin P, Barbezat M, Kausch HH. J Phys III (France) 1991;1:1867.
[17] Zuiderduin WCJ, Vlasveld DPN, Huétink J, Gaymans RJ. Polymer 2004;45:3765.
[18] van der Wal A, Gaymans RJ. Polymer 1999;40:6067.
[19] Paul RD, Bucknall CB. Polymer blends. vol. 2. New York: Wiley; 2000.